Dynamics of Electron-Phonon Scattering: Crystal- and Angular-Momentum Transfer Probed by Resonant Inelastic X-Ray Scattering

M. Beye,* F. Hennies, M. Deppe, E. Suljoti, M. Nagasono, W. Wurth, and A. Föhlisch†

Institut für Experimentalphysik, Universität Hamburg and Centre for Free-Electron Laser Science, Hamburg, Germany

(Received 20 May 2009; published 2 December 2009)

Experimentally, we observe angular-momentum transfer in electron-phonon scattering, although it is commonly agreed that phonons transfer mostly linear momentum. Therefore, the incorporation of angular momentum to describe phonons is necessary already for simple semiconductors and bears significant implications for the formation of new quasiparticles in correlated functional materials. Separation of linear and angular-momentum transfer in electron-phonon scattering is achieved by highly selective excitations on the femtosecond time scale of resonant inelastic x-ray scattering.

DOI: 10.1103/PhysRevLett.103.237401 PACS numbers: 78.70.En, 63.20.kd, 71.20.Mq, 78.47.−p

The rich physics of functional materials is based on the interplay between electronic, nuclear, and spin excitations that form quasiparticle states of often amazingly different properties in comparison to the bare, undressed particles. Although the different subsystems, i.e., electrons, spins, or phonons, are well understood and simulated [1], their correlated interaction still bears surprises leading to spectacular materials properties, phase transitions, and ultra fast switching phenomena. For example, the combination of electronic and phononic excitations are responsible for conventional superconductivity [2] and the explanation of high temperature superconductivity presumably needs coupling to another subsystem [3]. In this work, we focus on crystalline silicon—a simple, uncorrelated semiconductor—and address the question how angular and crystal momentum is transferred in electron-phonon scattering. Our quantitative insight into this basic process can then be used to particularize our understanding of more complicated systems.

Experimentally, we use the symmetry selection rules of resonant inelastic x-ray scattering (RIXS) that allow us to determine electron-phonon scattering processes that lead to crystal and angular-momentum transfer separately. In a first step, we quantify the k conservation and k transfer in thermally equilibrated crystalline silicon at temperatures ranging from room temperature up to the melting point. Then, the transfer of orbital angular-momentum under equivalent temperature conditions is selectively determined. Since we control the sample temperature and through the excitation energy the RIXS duration time [4–7], we extract the electron-phonon scattering rate without distorting matrix element effects. Whereas in previous work only the k conservation and k transfer in RIXS on crystalline materials was considered [7–14] and the possible existence of plasmon and phonon states with finite orbital angular momentum has just started to be debated [15], we present quantitative experimental evidence of significant angular-momentum transfer in electron-phonon scattering. In particular, both the crystal and angular-momentum transfer rates depend on temperature proportional to the increasing phonon number. In addition, we find for temperatures close to the silicon melting point also sizeable contributions due to electron-electron interaction, which contribute significantly to the transfer of crystal momentum, but do not transfer angular momentum.

The experiment was performed at beam line UE52-PGM at BESSY II, Germany. At pressures below 10^{-9} mbar, we flashed weakly Boron-doped Si (100) samples to remove the surface oxide. Cleanliness was ensured by photoelectron spectroscopy. Emission spectra were recorded with a Scienta XES355 soft-x-ray spectrometer [6] in the plane of the incident polarization. The silicon sample was heated resistively, and the temperature was recorded pyrometrically. The excitation bandwidth was set to 100 meV, whereas the soft-x-ray spectrometer was operated at 400 meV resolution.

In Fig. 1, the evolution of the RIXS spectral profiles as a function of sample temperature (300 –1550 K) and excitation energy across and above the Si L_3 absorption edge is shown [16]. Based on this systematic variation of photon energy and sample temperature, we can quantify the electron-phonon scattering processes leading to crystal momentum transfer and to angular-momentum transfer, highlighting the most relevant features in Figs. 2 and 3, respectively.

In Fig. 2, we concentrate on the role of crystal momentum transfer in electron-phonon scattering. In Fig. 2(a), we depict schematically how the k conservation in RIXS is influenced. For RIXS without electron-phonon scattering, the narrow bandwidth resonant excitation creates a core excited state at a well-defined point in k space. Since soft-x-ray photons carry negligible momentum, k conservation in the RIXS process allows radiative decay from the same point in the Brillouin zone only [12,13,17,18]. Thus, we observe valence-band-hole–conduction-band-electron final states at this selected k value only. In the experimental spectrum measured for resonant excitation into the conduction band minimum (CBM) at room temperature [Fig. 2(b)], we observe thus a clear relationship between the k value of the CBM and the discrete RIXS spectral

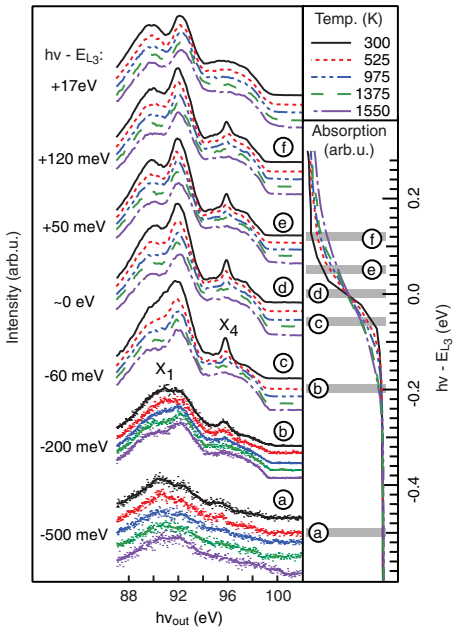

FIG. 1 (color online). Left: Si $2p$ RIXS at different temperatures and excitation energies. The elastic scattering peak has been removed. Intensities are shifted for each spectrum. Right: absorption spectra on a common photon energy scale, the respective inflection point is set to zero. Grey bars indicate the position of the excitation energies in RIXS.

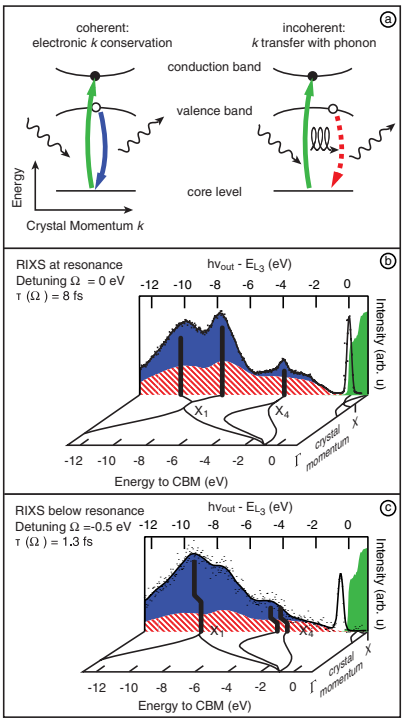

FIG. 2 (color online). (a) k conservation in RIXS (left) and crystal momentum transfer due to electron-phonon scattering in RIXS (right). (b) Threshold excitation into the CBM (light shaded, green: absorption): The RIXS spectrum consists of k-selective coherent features (dark shaded, blue) and the incoherent fraction (red hatched). The elastic scattering peak is also shown. (c) Detuned excitation 500 meV below the CBM (light shaded, green: absorption): Reduced RIXS duration times suppresses the incoherent fraction (red hatched).

features (black lines), that represent a cut through the valence band structure at this selected k value. This part of the spectra is called the coherent part (dark area, blue) and has three distinct peaks, reflecting the electronic bands at the selected k value.

In addition to these k-conserving features, we observe a broad incoherent contribution (hatched area), that is caused by electron-phonon scattering, redistributing crystal momentum between the core excited state and the phononic system during the Si $2p_{3/2}$ core-hole lifetime of 8 fs [12]. It reflects thus the k-integrated density of states (DOS) and resembles to a good approximation the nonresonant emission spectral profile for continuum excitation, where any crystal momentum value is visible in radiative decay (Fig. 1 top).

At identical resonant excitation conditions, we observe for increasing sample temperature a reduction of the k-conserving coherent fraction and a gain in the incoherent fraction [see, e.g., Fig. 1 (d)]. We can also change the photon energy and detune the excitation energy off resonance by the detuning energy $\Omega = h\nu - E_{L_3}$. Detuning has two effects: It will change the selected k values in the scattering process, and—inseparably—the effective RIXS duration time $\tau(\Omega)$ will be shortened [19]. In detail, the effective scattering duration time follows $\tau(\Omega) = \hbar(\Omega^2 + \Gamma^2)^{-1/2}$ [5], where the lifetime of the core excited intermediate state is expressed in its natural lifetime broadening Γ (HWHM). For resonant Si $2p_{3/2}$ core excitation into the CBM, the effective RIXS duration time corresponds to $\tau(\Omega = 0\ \text{eV}) = 8$ fs [12] and shortens for detuned excitation to $\tau(\Omega = -0.5\ \text{eV}) = 1.3$ fs. Detuning the excitation energy strengthens the coherent fraction relative to the incoherent fraction, since the probability for the occurrence of an electron-phonon scattering event during the shorter effective RIXS duration time is reduced [see Fig. 2(c)].

Based on these considerations, we quantify the electron-phonon scattering rate R_{ph} that leads to a change of crystal momentum. Since a single electron-phonon scattering event transfers sufficient momentum to change the initially selected k-value of the core excited state randomly across the whole Brillouin zone, the ratio of the phonon scattering rate and the decay rate (i.e., the inverse of the effective RIXS duration time) equal to the ratio of RIXS events with phonon scattering and those without, becomes visible in the ratio of the incoherent and the coherent intensity contributions [20].

In Fig. 4(a), we summarize our analysis of the k transferring electron-phonon scattering rate R_{ph} as a function of temperature, taking the coherent and incoherent fractions of RIXS as well as the effective scattering time into account.

Before we discuss Fig. 4 in detail, we will turn to the influence of angular momentum transfer in electron-

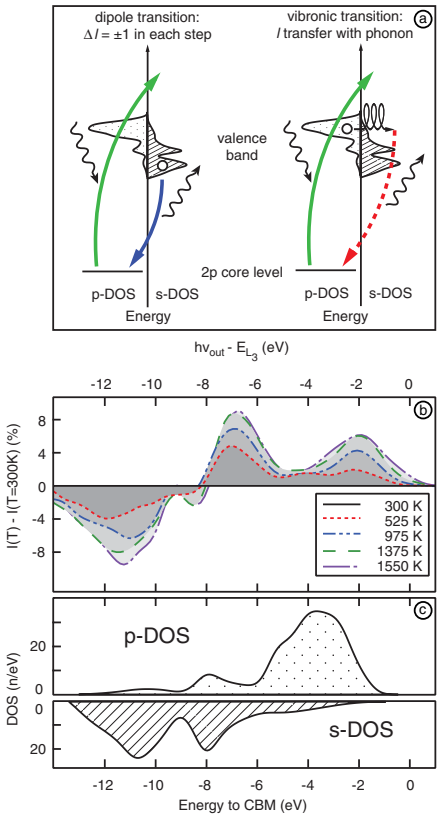

FIG. 3 (color online). (a) Left: Electronic dipole transitions obey $\Delta l = \pm 1$. A $2p$ core hole is created (green) and filled from valence s states (blue). Right: The $2p$ core hole can be filled from a valence p state when a phonon with $|l| = 1$ is created or absorbed (curly line). The energy of the radiative transition (red) then reflects the p DOS. (b) Relative difference of the nonresonant excited emission spectra at different temperatures and the 300 K spectrum. (c) Calculated partial DOS of silicon. The s partial DOS is shown inverted. Contributions from other symmetries to the DOS are negligible.

phonon scattering as presented in Fig. 3. To observe this effect, we have to find a way to be experimentally sensitive to angular-momentum transfer only. This situation exists for nonresonant excitation above the ionization threshold, where k transfer does not affect the spectral distribution, since the dispersionless core-ionized intermediate state contains already all k values of the Brillouin zone. The orbital angular-momentum features of electronic bands are accessible in RIXS because here the projection on a core-level wave function is measured, where the orbital angular momentum is well defined.

Atomic symmetry selection rules apply, and the electronic decay of the Si $2p$ core-hole state probes in the dipole approximation the s valence partial DOS of silicon. In contrast, the electronic decay of the p valence partial DOS is forbidden, but can be enabled through angular-momentum transfer occurring in electron-phonon scattering (in molecules this is called a vibronic transition [4], where the angular momentum of the nuclear wave function is changed accompanying the electronic transition).

In Fig. 3(a), we show a cartoon how angular-momentum transfer in electron-phonon scattering enables symmetry forbidden electronic radiative p-p decay, which we then use as a measure of the phonon-induced angular-momentum transfer in silicon.

As a function of sample temperature, the relative contributions from the s and p partial DOS change significantly. In Fig. 3(b), the temperature dependent difference from the room temperature spectral distribution of the nonresonantly excited emission spectra of silicon is shown. Differences are normalized to the highest intensity in the room temperature spectrum. In direct comparison, we present the orbital symmetry resolved partial density of states, calculated for $T = 0$ K and broadened to mimic the experimental resolution [Fig. 3(c)] [21].

We observe how increasing temperature shifts spectral weight from the s to p valence states. This shift is a signature of angular-momentum transfer through phonons, as it evolves with temperature. With a simple model, where a scattering event during the core excited state lifetime changes the symmetry, we evaluate the l transferring phonon scattering rate from the respective contributions to the measured spectra as estimated by fitting with a superposition of the calculated s and p DOS [22]. The results as a function of temperature are shown in Fig. 4(b).

We can now discuss in Fig. 4 the thermal evolution of the k and l transferring phonon scattering rates. We observe a constant contribution due to phonons created by core excited state lattice distortions. The temperature dependent part of the scattering rates is proportional to the phonon number, modeled by a Bose-Einstein function for a single phonon mode with 38 meV energy [23]. We find electron-phonon scattering rates per thermally excited average pho-

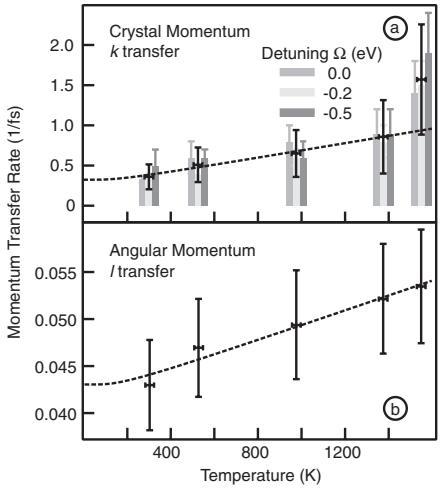

FIG. 4. (a) The k-transferring electron-phonon scattering rate as a function of detuning and temperature. Averaged values are shown solid black along with a fit to the Bose-Einstein distribution function up to 1375 K. (b) The l-transferring electron-phonon scattering rate as a function of temperature. The fit is performed including all data points. Note the different scales on the ordinate.

non of $0.20(2) \times 10^{15}/\mathrm{s}$ for the k transfer and $0.0035(4) \times 10^{15}/\mathrm{s}$ for the l transfer. This shows that the probability to transfer crystal momentum from a phonon to an electron is more than 50 times higher than an angular-momentum transfer. This might be the reason why this contribution has so far been neglected. We conclude that nearly every phonon carries significant crystal momentum, but only few of them possess a nonzero angular momentum. Please note that the reported value for the electron-phonon scattering rate complements the results from experiments with short laser pulses [24].

An influence of electron-electron coupling becomes visible in Fig. 4(a) at 1550 K. The k transfer is much bigger than expected from the thermal increase in phonon scattering. This is due to the k transfer through scattering with thermally excited electrons in the intermediate core-hole–CBM-electron state. The situation differs for the l transfer as seen at 1550 K in Fig. 4(b). We observe no additional l transfer at high temperatures as electron-electron scattering cannot influence the core-ionized intermediate state.

In conclusion, we determine the electron-phonon coupling properties of silicon between room temperature and the melting point through RIXS at the L_3 edge. We separately analyze the accompanying crystal and angular-momentum transfer and find scattering rates per thermally excited average phonon of $0.20(2) \times 10^{15}/\mathrm{s}$ for the k transfer and $0.0035(4) \times 10^{15}/\mathrm{s}$ for the l transfer. Therefore, we conclude that around 2% of the thermally excited phonons carry a nonzero angular momentum. Additionally, we find a temperature independent contribution from phonons created through core excited state lattice distortions.

This work was supported by the Deutsche Forschungsgemeinschaft (Grant DFG Fo343/1-2). Valuable support from BESSY staff is gratefully acknowledged.

*Corresponding author: martin.beye@desy.de
†Corresponding author: alexander.foehlisch@helmholtz-berlin.de;
Present address: Helmholtz-Zentrum Berlin and University of Potsdam, Germany.

[1] S. Baroni, S. de Gironcoli, A. Dal Corso, and P. Giannozzi, Rev. Mod. Phys. **73**, 515 (2001).
[2] J. Bardeen, L. N. Cooper, and J. R. Schrieffer, Phys. Rev. **108**, 1175 (1957).
[3] M. Capone, M. Fabrizio, C. Castellani, and E. Tosatti, Science **296**, 2364 (2002).
[4] F. Hennies, S. Polyutov, I. Minkov, A. Pietzsch, M. Nagasono, F. Gel'mukhanov, L. Triguero, M.-N. Piancastelli, W. Wurth, and H. Agren *et al.*, Phys. Rev. Lett. **95**, 163002 (2005).
[5] F. Gel'mukhanov and H. Ågren, Phys. Rep. **312**, 87 (1999).
[6] J. Nordgren and J. Guo, J. Electron Spectrosc. Relat. Phenom. **110–111**, 1 (2000).
[7] A. Kotani and S. Shin, Rev. Mod. Phys. **73**, 203 (2001).
[8] Y. Ma, K. E. Miyano, P. L. Cowan, Y. Aglitzkiy, and B. A. Karlin, Phys. Rev. Lett. **74**, 478 (1995).
[9] J. A. Carlisle, E. L. Shirley, E. A. Hudson, L. J. Terminello, T. A. Callcott, J. J. Jia, D. L. Ederer, R. C. C. Perera, and F. J. Himpsel, Phys. Rev. Lett. **74**, 1234 (1995).
[10] S. Shin, A. Agui, M. Watanabe, M. Fujisawa, Y. Tezuka, and T. Ishii, Phys. Rev. B **53**, 15660 (1996).
[11] S. Eisebitt, J. Lüning, J.-E. Rubensson, A. Settels, P. H. Dederichs, W. Eberhardt, S. N. Patitsas, and T. Tiedje, J. Electron Spectrosc. Relat. Phenom. **93**, 245 (1998).
[12] S. Eisebitt and W. Eberhardt, J. Electron Spectrosc. Relat. Phenom. **110–111**, 335 (2000).
[13] A. V. Sokolov, L. D. Finkelstein, E. Z. Kurmaev, S. Shin, P. F. Karimov, N. A. Skorikov, and A. V. Postnikov, J. Electron Spectrosc. Relat. Phenom. **137**, 591 (2004).
[14] V. N. Strocov, T. Schmitt, J.-E. Rubensson, P. Blaha, T. Paskova, and P. O. Nilsson, Phys. Rev. B **72**, 085221 (2005).
[15] J. T. Mendonça, B. Thidé, and H. Then, Phys. Rev. Lett. **102**, 185005 (2009).
[16] We define the excitation energy scale relative to the turning point of the Si L_3 absorption edge: $h\upsilon - E_{L_3} = 0$.
[17] Y. Ma, N. Wassdahl, P. Skytt, J. Guo, J. Nordgren, P. D. Johnson, J.-E. Rubensson, T. Boske, W. Eberhardt, and S. D. Kevan, Phys. Rev. Lett. **69**, 2598 (1992).
[18] M. van Veenendaal and P. Carra, Phys. Rev. Lett. **78**, 2839 (1997).
[19] P. F. Williams, D. L. Rousseau, and S. H. Dworetsky, Phys. Rev. Lett. **32**, 196 (1974).
[20] We separate the sharp features of the coherent part, stemming from single points in the band structure and the broad incoherent part as modeled with the nonresonantly excited spectrum, by scaling the latter as high as possible inside the measured spectra. Ambiguities in this procedure determine the error bars in Fig. 4(a). The intensity ratio connects then as follows:
$$\frac{I_{\mathrm{inc}}}{I_{\mathrm{coh}}} = \tau(\Omega) R_{\mathrm{ph}}.$$
[21] We use data from the Japanese National Institute for Materials Science database (http://caldb.nims.go.jp).
[22] In contrast to continuous k transfer, an even number of $|l| = 1$ transfers will result in the same state (omitting states with $l \geq 2$ because of vanishing DOS). Combining the probability for a core-hole decay at time t, $\exp(-t/\tau)$, with the probability that a single phonon scattering event (rate R) has not yet happened, $1 - \exp(-Rt)$, including multiphonon scattering with alternating sign, yields for the s-like contribution to the spectra:
$$I_s = \int_0^\infty \frac{\exp(-t/\tau)}{\tau} \left(\sum_{n=0}^{\infty} (-1)^n [1 - \exp(-Rt)]^n \right) dt = \int_0^\infty \frac{\exp(-t/\tau)}{\tau[2 - \exp(-Rt)]} dt.$$
[23] R. Pässler, Phys. Status Solidi B **236**, 710 (2003).
[24] A. J. Sabbah and D. M. Riffe, Phys. Rev. B **66**, 165217 (2002).